Acta Oceanol. Sin., 2018, Vol. 37, No. 12, P. 97–106
DOI: 10.1007/s13131-018-1342-x
http://www.hyxb.org.cn
E-mail: hyxbe@263.net

Phytoplankton pigment pattern in the subsurface chlorophyll maximum in the South Java coastal upwelling system, Indonesia

GAO Chunlei[1, 2, 3†], FU Mingzhu[1, 2, 3*†], SONG Hongjun[1, 2, 3], WANG Lei[4], WEI Qinsheng[1, 2, 3], SUN Ping[1, 2, 3], LIU Lin[1], ZHANG Xuelei[1, 2, 3]

[1] First Institute of Oceanography, Ministry of Natural Resources, Qingdao 266061, China

[2] Laboratory of Marine Ecology and Environmental Science, Pilot National Laboratory for Marine Science and Technology (Qingdao), Qingdao 266237, China

[3] Key Laboratory of Science and Engineering for Marine Ecological Environment, Ministry of Natural Resources, Qingdao 266061, China

[4] Third Institute of Oceanography, Ministry of Natural Resources, Xiamen 361005, China

Received 4 January 2018; accepted 1 February 2018

Abstract

Upwelling occurs on the coast of Java between June and October, forced by local alongshore winds associated with the southeasterly monsoon. This causes variations in phytoplankton community composition in the upwelling zone compared with the surrounding offshore area. Based on pigments analysis with subsequent calculations of group contributions to total chlorophyll *a* (Chl *a*) using CHEMTAX, we studied the distribution and composition of phytoplankton assemblages in the subsurface chlorophyll maximum along the south coast of Java and the influence of upwelling. Nineteen phytoplankton pigments were identified using high-performance liquid chromatography, and CHEMTAX analysis associated these to ten major phytoplankton groups. The phytoplankton community in the coastal area influenced by upwelling was characterized by high Chl *a* and fucoxanthin concentrations, indicating the dominance of diatoms. In contrast, in the offshore area, the Chl *a* and fucoxanthin concentrations declined to very low levels and the community was dominated by haptophytes represented by 19′-Hexanoyloxyfucoxanthin. Accordingly, microphytoplankton was found to be the major size class in the coastal area influenced by upwelling, while nanophytoplankton was most abundant in the offshore area. Low concentrations of other accessory pigments indicated less contribution from dinoflagellates, prasinophytes, chlorophytes and cryptophytes. Photo-pigment indices revealed that photosynthetic carotenoids (PSCs) were the largest component of the pigment pool, exceeding the proportion of Chl *a*, with the average PSC_{TP} up to 0.62. These distribution trends can mainly be explained by phytoplankton adaption strategies to upwelling and subsurface conditions by changing species composition and adjusting the pigment pool.

Key words: Java upwelling, phytoplankton pigment, HPLC, subsurface chlorophyll maximum, CHEMTAX, size structure

Citation: Gao Chunlei, Fu Mingzhu, Song Hongjun, Wang Lei, Wei Qinsheng, Sun Ping, Liu Lin, Zhang Xuelei. 2018. Phytoplankton pigment pattern in the subsurface chlorophyll maximum in the South Java coastal upwelling system, Indonesia. Acta Oceanologica Sinica, 37(12): 97–106, doi: 10.1007/s13131-018-1342-x

1 Introduction

Marine phytoplankton is a taxonomically and functionally diverse group of organisms that are key players in the most important biogeochemical cycles (Bonachela et al., 2016). They are the most abundant and widespread primary producers in the world's oceans and support a bulk of marine food webs (Paerl and Justić, 2011). Because of the important global role of phytoplankton, monitoring their biomass and species composition has become a high priority of oceanographic research (Jeffrey et al., 2011). Pigment analysis is a powerful chemotaxonomic method to detect phytoplankton abundance and composition. Rapid, precise analysis can be carried out routinely to measure phytoplankton in all size ranges (Schlüter et al., 2011). It is particularly useful in oligotrophic areas where nano- and pico-planktonic organisms prevail; these are normally unrecognizable by light microscopy, and are often difficult to preserve (Wright and Jeffery, 2006; Higgins et al., 2011). Monitoring phytoplankton by the pigment method has been conducted in open oceans (e.g., Gibb et al., 2000; Barlow et al., 2007, 2016; Ras et al., 2008; Schlüter et al., 2011; Araujo et al., 2017) and coastal areas (e.g., Chai et al., 2016; Mendes et al., 2016; Isada et al., 2017).

Sumatra and Java in Indonesia are located in the Indian Ocean warm pool, and form part of the eastern boundary of the tropical Indian Ocean (Horii et al., 2016). Seasonally varying monsoon winds over the Indonesian region have a great impact on the pattern of oceanic circulation along the southern coasts of

Foundation item: The Global Change and Air-Sea Interaction Program under contract Nos GASI-02-IND-ST-Sspr and GASI-03-01-03-03; the National Natural Science Foundation of China under contract No. 41506185; the Special Funds for Basic Ocean Science Research of the First Institute of Oceanography, State Oceanic Administration of China under contract Nos 2013T04 and 2012T08.
*Corresponding author, E-mail: fumingzhu@fio.org.cn
†These authors contributed equally to this work.

Java and Sumatra (Wyrtki, 1962; Iskandar et al., 2009). During the southeast monsoon, the prevailing southeasterly winds from Australia drive offshore Ekman transport and generate upwelling off Java. This starts in June, reaches its peak in August and diminishes in October–November due to the reversal of winds (Susanto et al., 2001). In addition to monsoon winds, the Indonesian Throughflow (ITF) may also play an important role in the formation of the East Java upwelling (Kuswardani and Qiao, 2014). The upwelling brings cooler and nutrient-rich water to the ocean surface, supporting high primary production and making this area the site of important fisheries (Susanto and Marra, 2005; Sartimbul et al., 2011). The chlorophyll *a* (Chl *a*) concentration during the southeasterly monsoon off the South Java coast is higher than that during the northwesterly monsoon season (Susanto and Marra, 2005). The variation in phytoplankton blooms induced by the upwelling along the coast of Java has been reported mostly through remote sensing and numerical models (Reddy and Salvekar, 2008; Iskandar et al., 2009, 2010). To our knowledge, the information of phytoplankton community structure in this monsoonal upwelling system is fairly limited.

Based on field observations during September–October 2013, we studied phytoplankton pigment distribution along the southern coast of Java, Indonesia, during the decay of an upwelling event. The aims of our study were: (1) to identify the major phytoplankton groups off the south coast of Java; and (2) to study the influence of the upwelling on the phytoplankton community structure.

2 Materials and methods

2.1 *Study area and water sampling*

The study area is located at 7°–10°S, 106°–114°E in the eastern tropical Indian Ocean near the coast of Java, Indonesia (Fig. 1). Besides the southeasterly wind-induced upwelling, the study area is also affected by the South Java Current (SJC) and the ITF.

Our investigation was conducted from 22 September to 2 October 2013 on board the R/V *BJ*–8 from the Indonesian Institute of Sciences (in Indonesian: Lembaga Ilmu Pengetahuan Indonesia or LIPI), Indonesia. Twelve stations belong to two transects perpendicular to the coast were occupied.

Profiles of seawater temperature, salinity and fluorescence were obtained with a SeaBird 911 CTD equipped with pre-calibrated fluorescence sensor (SeaBird Inc., Bellevue, WA, USA). At each station, water samples for nutrient analysis (nitrate, phosphate, silicate) and picophytoplankton cell abundance were collected at depths of 3 m, 10 m, 30 m, 50 m, 75 m, 100 m, 150 m, 200 m and 300 m with 10-L Niskin bottles mounted on CTD. Water samples (3 L) for the analysis of phytoplankton pigments were only collected at the depth of subsurface chlorophyll maximum (SCM). Water samples were filtered in dim light through Whatman GF/F filters (nominal pore size 0.7 μm and 25 mm diameter), and immediately frozen in liquid nitrogen for later high-performance liquid chromatography (HPLC) pigment analysis.

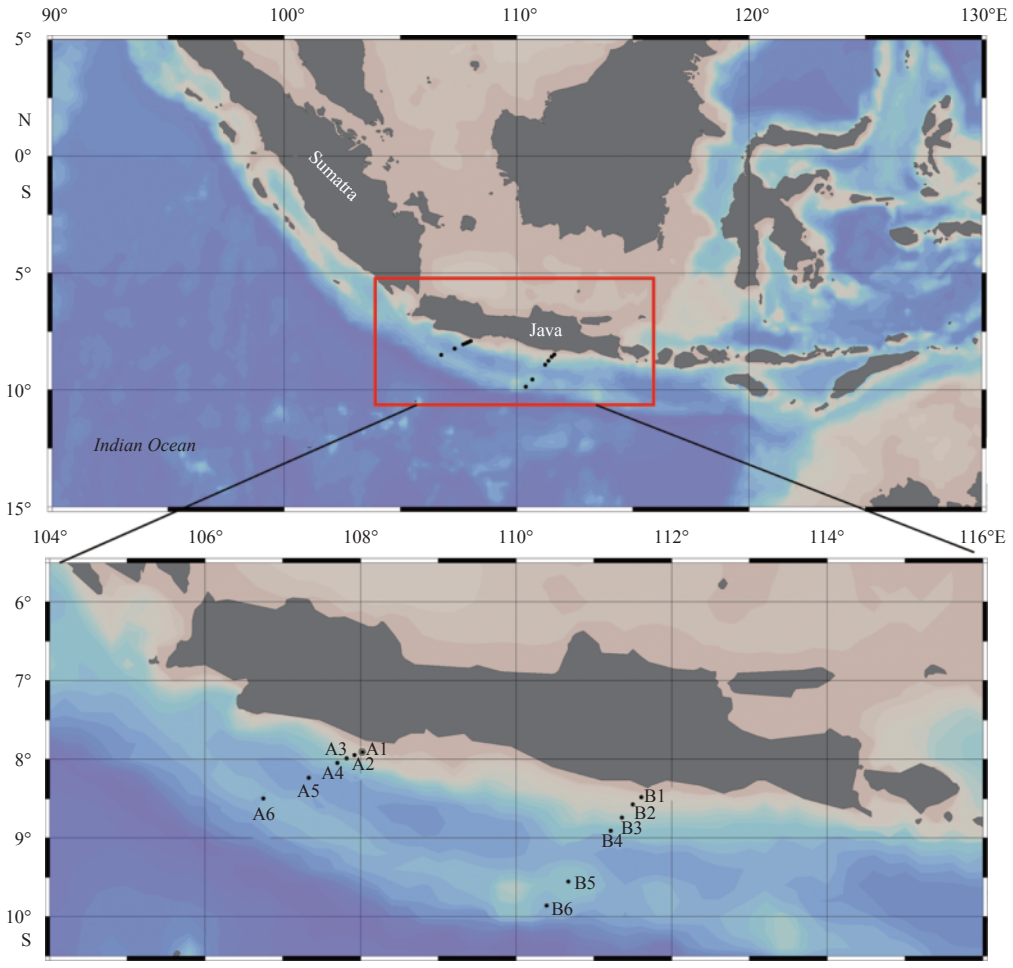

Fig. 1. Study area and sampling stations.

2.2 *Chemical measurements*

Five hundred milliliter of seawater was filtered through GF/F filters and the filtrate was immediately stored at –20°C until analysis at the land laboratory. Concentrations of nitrate, phosphate and silicate were measured by the spectrophotometry method provide by Grasshoff et al. (1999). The standard deviations were 0.05 μmol/L for nitrate, 0.02 μmol/L for phosphate and 0.05 μmol/L for silicate.

2.3 *HPLC analysis*

The entire extraction procedure was carried out in subdued light and at low temperature to minimize degradation of pigments. The filters were cut into 0.5 cm×0.5 cm pieces and put into a Teflon-lined screw-capped syringe with 5 mL 100% methanol containing 0.025 mg/mL vitamin E acetate as internal standard. The filters were then sonicated in the syringes for 10 s (Schlüter et al., 2011) in a ultrasonic processor (XHF-D, Ningbo Scientz Biotechnology), and filtered through 13 mm diameter PP-syringe filters to remove cell and filter debris. An aliquot (700 μL) of methanol extract was mixed with 140 μL of water in an HPLC vial to avoid the shape distortion of earlier eluting peaks (Zapata and Garrido, 1991). The vials were placed in the cooling rack (4°C) of the HPLC autosampler and immediately analysed following the method of Zapata et al. (2000) using a monomeric C8 column (Waters Symmetry C8, 150 mm×4.6 mm, 3.5 μm particle size) with pyridine as a solvent modifier. The Waters 600 HPLC system was employed for the analysis. This consisted of a Waters 600 Controller, Waters 2998 Photodiode Array Detector, Waters 2475 Multi-Fluorescence Detector, and a Waters 717 plus Autosampler equipped with a temperature control module and a column oven (M500, PX Science and Technology, Tianjin, China). Before analysis, the HPLC system was calibrated with pigment standards from DHI (Institute for Water and Environment, Denmark) and calibration curves were established for response factors of each pigment. Phytoplankton pigments were identified from both absorbance spectra and retention times from the signals in the photodiode array detector (Waters 1998, 350–750 nm, 1.2 nm spectral resolution) or fluorescence detector (Waters 2475, Ex: 440 nm, Em: 650 nm). Absorbance chromatograms were extracted at 430, 440 and 450 nm. The internal standard was detected at 220 nm. Pigments were quantified by the internal standard and response factor of each pigment. The concentrations of pigments without standards were determined according to the response factors of their homogenous pigments.

2.4 *Pigment indices*

Photo-pigment indices were derived to assess the different contribution of chlorophylls and carotenoids to the total pigment pool. The carotenoids were distinguished as photosynthetic carotenoids (PSCs) and photoprotective carotenoids (PPCs). The PSCs included 19′-butanoyloxyfucoxanthin, fucoxanthin, 19′-hexanoloxyfucoxanthin and peridinin; the PPCs were composed of alloxanthin, ββ- + βε-carotene, diadinoxanthin, diatoxanthin, lutein, violaxanthin and zeaxanthin (Barlow et al., 2007).

We also constructed the pigment-based size classes proposed by Vidussi et al. (2001) and improved by Uitz et al. (2006) using the weighted sum of seven diagnostic pigments (Table 1). The sum of all weighted diagnostic pigments, ΣDPw, was ex-

Table 1. Pigments determined, their abbreviations and designations, pigment sums and pigment indices in this study

Abbreviation	Pigment	Designation
Chl *a*	chlorophyll *a*	
Chl *b*	chlorophyll *b*	Chlorophytes
Chl c_2	chlorophyll c_2	
Chl c_3	chlorophyll c_3	
Chlidea	chlorophyllide *a*	
DVChl *a*	divinyl chlorophyll *a*	Prochlorophytes
Allo	alloxanthin	Crptophytes
But	19′-butanoyloxyfucoxanthin	Pelagophytes (major) Haptophytes (secondary)
Caro	ββ-carotene + βε-carotene	
Diad	diadinoxanthin	
Diato	diatoxanthin	
Fuco	fucoxanthin	Diatoms (major)
Lut	lutein	
Hex	19′-hexanoyloxyfucoxanthin	Haptophytes
Neox	neoxanthin	
Peri	peridinin	Dinoflagellates
Pras	prasinoxanthin	Prasinophytes
Viol	violaxanthin	
Zea	zeaxanthin	Cynobacteria
	Pigment sum	Formula
TChl *a*	total chlorophyll *a*	Chl *a* + DVChl *a* + Chlidea
PPC	photoprotective carotenoids	Allo + Caro + Diad + Diato + Lut + Viol + Zea
PSC	photosynthetic carotenoids	But + Fuco + Hex + Per
TP	total pigments	TChl *a* + Chl *b* + Chl c_2 + Chl c_3 + PPC + PSC
DP	diagnostic pigments	PSC + Allo + Chl *b* + Zea
	Pigment index	Formula
TChl a_{TP}	total chlorophyll *a* to total pigments	TChl *a*/TP
PPC_{TP}	photoprotective carotenoids to total pigments	PPC/TP
PSC_{TP}	photosynthetic carotenoids to total pigments	PSC/TP

pressed as

$$\Sigma\mathrm{DPw}= 1.41\,[\mathrm{Fuco}] +1.41\,[\mathrm{Peri}] +1.27\,[\mathrm{Hex}] +0.35\,[\mathrm{But}] + 0.60\,[\mathrm{Allo}] +1.01\,[\mathrm{Chl}\ b] +0.86\,[\mathrm{Zea}]\,. \quad (1)$$

The fractions of the Chl *a* concentration associated with each of the three phytoplankton classes (f_{micro}, f_{nano} and f_{pico}) were calculated as follows:

$$f_{\mathrm{micro}}= (1.41\,[\mathrm{Fuco}] +1.41\,[\mathrm{Peri}])\,/\Sigma\mathrm{DPw}, \quad (2)$$

$$f_{\mathrm{nano}}= (1.27\,[\mathrm{Hex}] +0.35\,[\mathrm{But}] +0.60\,[\mathrm{Allo}])\,/\Sigma\mathrm{DPw}, \quad (3)$$

$$f_{\mathrm{pico}}=1.01\,[\mathrm{Chl}\ b] +0.86\,[\mathrm{Zea}])/\Sigma\mathrm{DPw}. \quad (4)$$

2.5 *CHEMTAX*

The CHEMTAX program version 1.95 was used to calculate the Chl *a* biomass of the major phytoplankton groups. CHEMTAX uses a factor analysis and steepest-descent algorithm to find the best fit of the data to an initial pigment: Chl *a* ratios matrix (Mackey et al., 1996). In the present study, the initial pigment ratios for major algal classes were obtained from the literature (Higgins et al., 2011). Since the water samples were collected from the subsurface chlorophyll maximum depth, pigment values in the field studies under low light environments were chosen. The CHEMTAX input ratios were optimized with 60 further generated pigment ratios based on the method provided by Wright et al. (2009). The best 10% of results (n=6) with the lowest residual root mean square were chosen to calculate the average of the abundance.

3 Results

3.1 *Hydrographic and chemical conditions*

The hydrographic condition of the study area has been described in detail in Xue et al. (2016). Briefly, the water column was highly stratified, with temperature decreasing (salinity increasing) from the surface to the deep layer (Fig. 3 in Xue et al., 2016). The surface water temperature and salinity varied from 25.97°C to 27.85°C and from 33.71 to 34.27, respectively, in the sampling stations. In Transect A, we observed shoaling of temperature and salinity isolines towards the coast, which indicated the occurrence of the South Java coastal upwelling. The surface water was cooler (SST mean: 26.78°C) and more saline (SSS mean: 34.14) at the upwelling-influenced Stas A1 and A2 than at the offshore stations (A3–A6, SST mean: 27.67°C and SSS: 33.78). The hydrographic upwelling feature along Transect B was similar but not as clear as that along Transect A, although some researchers suggested Transect B was more affected by upwelling (Kuswardani and Qiao, 2014; Xue et al., 2016). At the SCM depth, water temperature and salinity varied from 23.32°C to 26.66°C and from 34.08 to 34.26, respectively.

The concentrations of nitrate, phosphate and silicate in surface waters along the two transects varied in the range of 0.05–0.29 μmol/L, 0.15–2.17 μmol/L and 4.00–6.80 μmol/L, respectively (Fig. 2). Silicate concentration was considerably greater than those of nitrate and phosphate. At the SCM depth the nutrient levels were just slightly higher, with concentrations of nitrate,

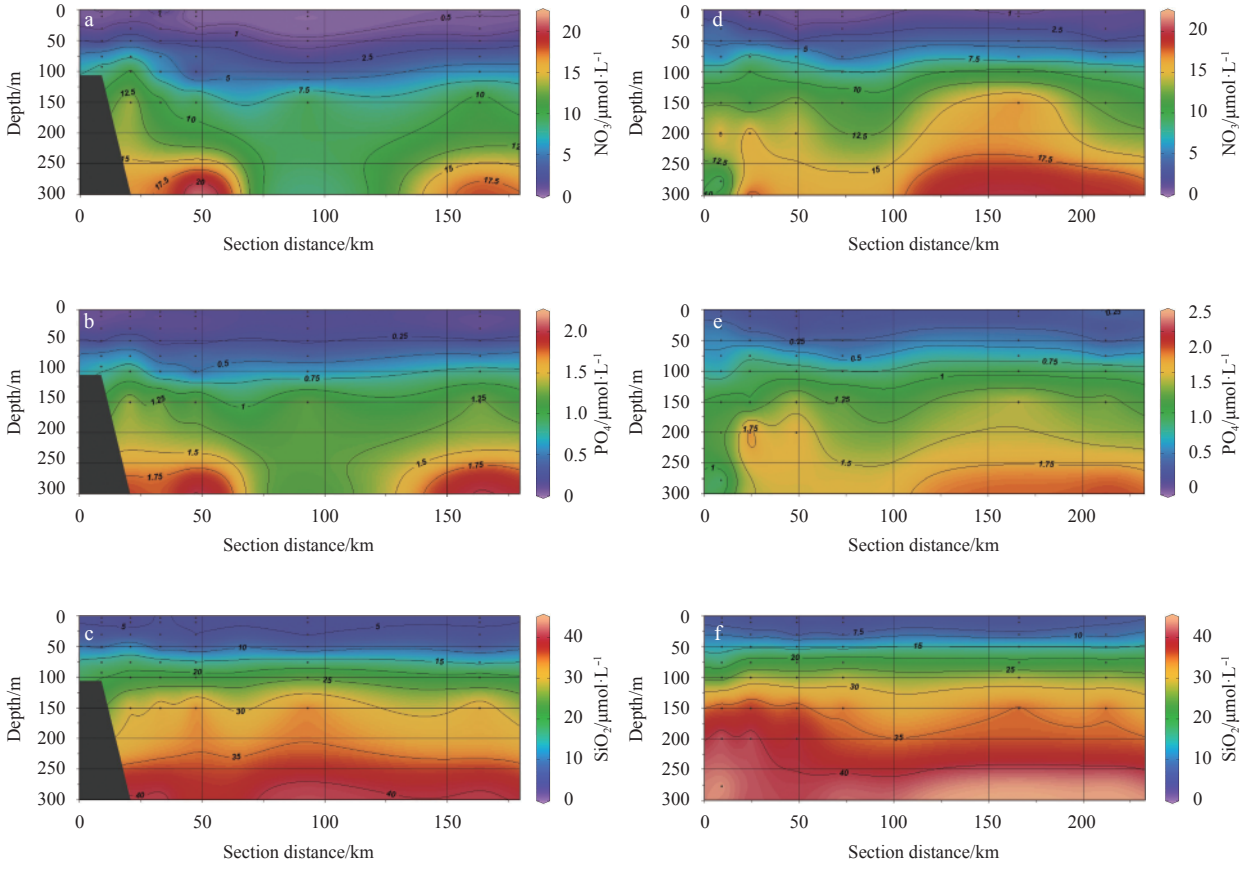

Fig. 2. Variation of nitrate, phosphate and silicate concentrations along Sections A (a, b, c) and B (d, e, f).

phosphate and silicate varying in the range of 0.02–0.34 μmol/L, 0.32–4.53 μmol/L and 4.20–15.2 μmol/L, respectively. This indicated that the vertical position of SCM was located at the upper boundary of the nutricline. In the present study, Stas A1, A2, B1 and B2 were defined as the coastal upwelling-influenced area.

3.2 *Phytoplankton pigment concentrations*

The pigments identified in the samples, and their abbreviations, are listed in Table 1. A total of 19 phytoplankton pigments including chlorophylls and caroteinods were identified in our study. The vertical profiles of the Chl *a* fluorescence sensor showed the SCM was generally present within a depth range of 30–50 m (Xue et al., 2016). The depth of SCM was elevated at Stas A1, A2, B1 and B2 due to the influence of upwelling. The concentrations of Chl *a* were significantly higher in coastal upwelling-influenced stations (29.30–191.15 ng/L) than at the offshore stations (9.86–22.16 ng/L) with the highest value recorded at Sta. B1.

The concentrations of accessory pigments also showed significant difference between the stations influenced by coastal upwelling and those offshore along the two transects (Fig. 3). The Fuco concentrations were distinctly different between the two regions: the average concentration was as high as 222.53 ng/L in the coastal upwelling area but decreased to only 4.20–18.06 ng/L in the offshore regions. In general, Hex (38.95–113.73 ng/L, with an average of 68.73 ng/L) and But (12.94–50.50 ng/L, with an average of 29.19 ng/L) were the dominant accessory pigments at the SCM in both transects and showed an increase trend from coast to offshore waters. DVChl *a*, the marker pigment of prochlorophytes, showed relatively high concentrations in the offshore area (6.68–11.64 ng/L), decreased to very low levels in Stas A1 and A2 (<2 ng/L) and was even absent in Stas B1 and B2. Zea was an important contributor to the accessory pigments along Transect B, following Hex and But, but was almost below the detection limit along Transect A except at Sta. A6. Compared with

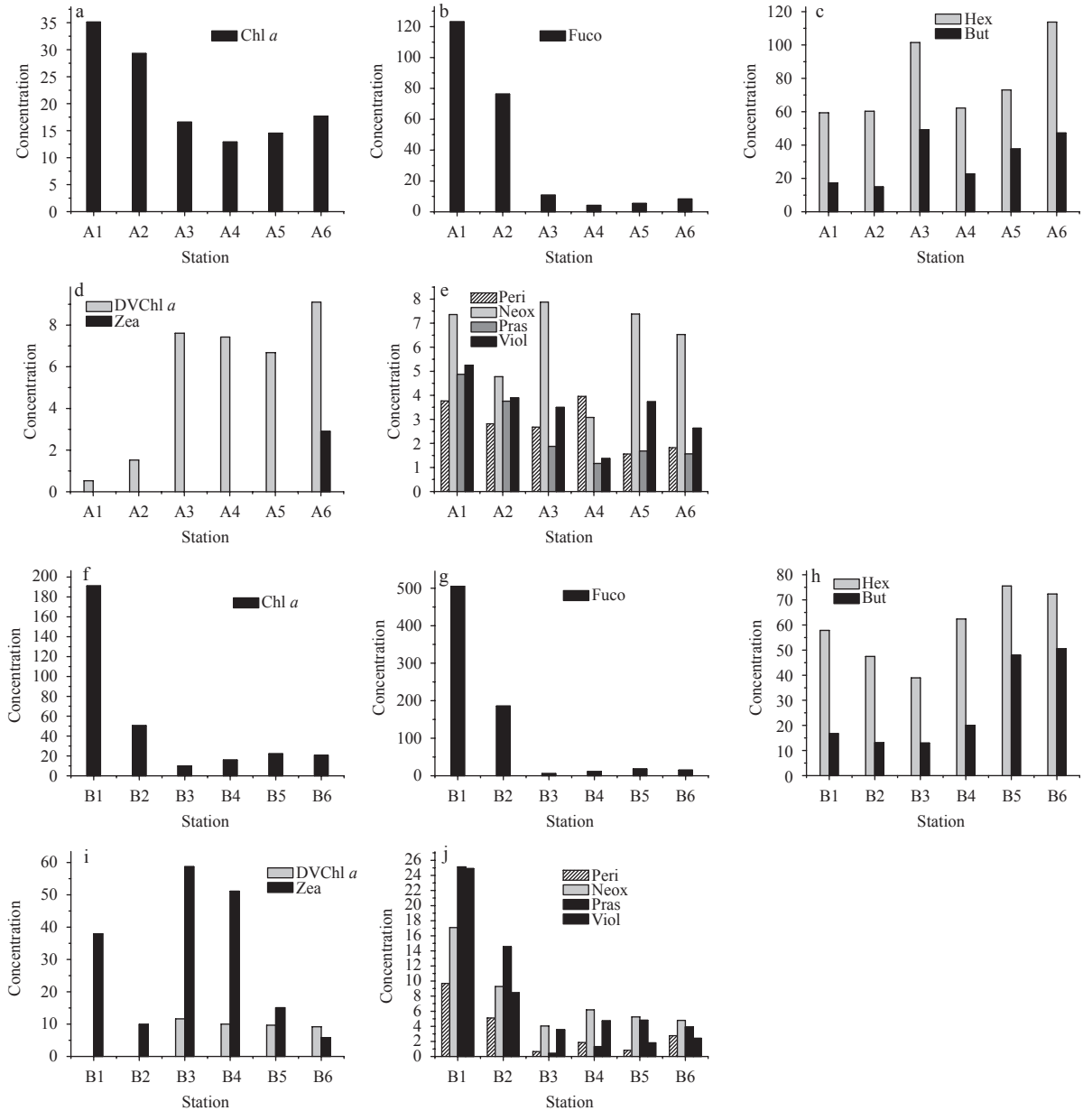

Fig. 3. Distribution of accessory pigments (ng/L) along Sections A (a–e) and B (f–j) at SCM. Pigment abbreviations are listed in Table 1.

these pigments, the concentrations of Peri, Pras, Neox and Viol were relatively low (<25 ng/L, most < 10 ng/L) and the concentrations of Allo and Lutein were extremely low (<2.5 ng/L). This indicated less contributions from dinoflagellates, prasinophytes, chlorophytes and cryptophytes.

3.3 *Pigment index*

The photopigment indices indicated that TChl a_{TP} was low and varied between 0.10 and 0.16 (with an average of 0.13) with small differences among the sampling stations (Fig. 4). The DVChl *a*/TChl *a* ratio, an index of the *Prochlorococcus* sp. contribution to TChl *a*, varied between 0 and 0.54 with an average of 0.23. DVChl *a* accounted for only a small fraction of total Chl *a* in the upwelling-influenced area (<5%), while accounting for 35.80% of total Chl *a* in the offshore area along the two transects.

PPC_{TP} was also low and varied between 0.09 and 0.45 (with an average of 0.16) with relatively elevated values observed at Stas B3 and B4. In Transect A, Diad was the major PPC, while in Transect B Zea was the predominant PPC.

PSCs were the largest component of the pigment pool, exceeding the proportion of Chl *a*; the average PSC_{TP} was up to 0.62. Among the PSCs, Fuco was the dominant contributor in the upwelling-influenced stations, while in the offshore stations Hex was the major contributor, followed by But.

The index of pigment-based size classes showed that the proportion of microphytoplankton (f_{micro}) was low (0.08–0.17, mean 0.11) throughout most of the sampling stations in the offshore areas but was significantly elevated at the coastal upwelling-influenced stations. As mentioned above, diatoms dominated in these first two stations along the transects with mean f_{micro} up to 0.72. Overall, nanophytoplankton was the major size class, contributing over 70% in the offshore stations along the two transects (Fig. 4). Picophytoplankton (f_{pico}) contribution was low and remained below 0.15 except in Stas B3 and B4.

3.4 *CHEMTAX-derived phytoplankton functional groups*

Based on the HPLC pigments data and the marker pigments characteristic of different microalgal taxa, thirteen pigments and ten taxonomic groups (pigment types) of phytoplankton were loaded for CHEMTAX analysis. The initial pigment ratios and output ratios from the CHEMTAX analyses are shown in Tables 2 and 3 respectively. Prochlorophytes, cryptophytes, dinoflagellates and prasinophytes were chosen for the presence of their unique diagnostic pigment of DVChl *a*, Allo, Peri and Pras, respectively. Diatoms, haptophyte type 8 and type 6 (Zapata et al., 2004), *Synecoccocus* and pelagophytes were chosen for the presence of their dominant accessory pigments of Fuco, Hex, Zea and But, respectively. The detection of Chl *b* indicated the possible presence of chlorophytes.

The phytoplankton groups calculated by CHEMTAX revealed that diatoms dominated in the upwelling-influenced stations but were only sporadically present in the offshore areas (Fig. 5). This has been confirmed by the microscopic examination results from the same cruise. In the upwelling-influenced stations, several species of diatoms, e.g., *Thalassiothrix longissima*, *Nitzschia* spp., *Odontella mobiliensis* and *Guinardia delicatula*, were identified as the dominant species (Sun Ping, personal communication). Overall, haptophyte type 8 dominated in the offshore areas while *Synecoccocus* also made an important contribution in the offshore area along Transect B. The average contribution of prochlorophytes was 11.10%, primarily distributed in the offshore stations. Prasinophytes presented in all sampled stations with

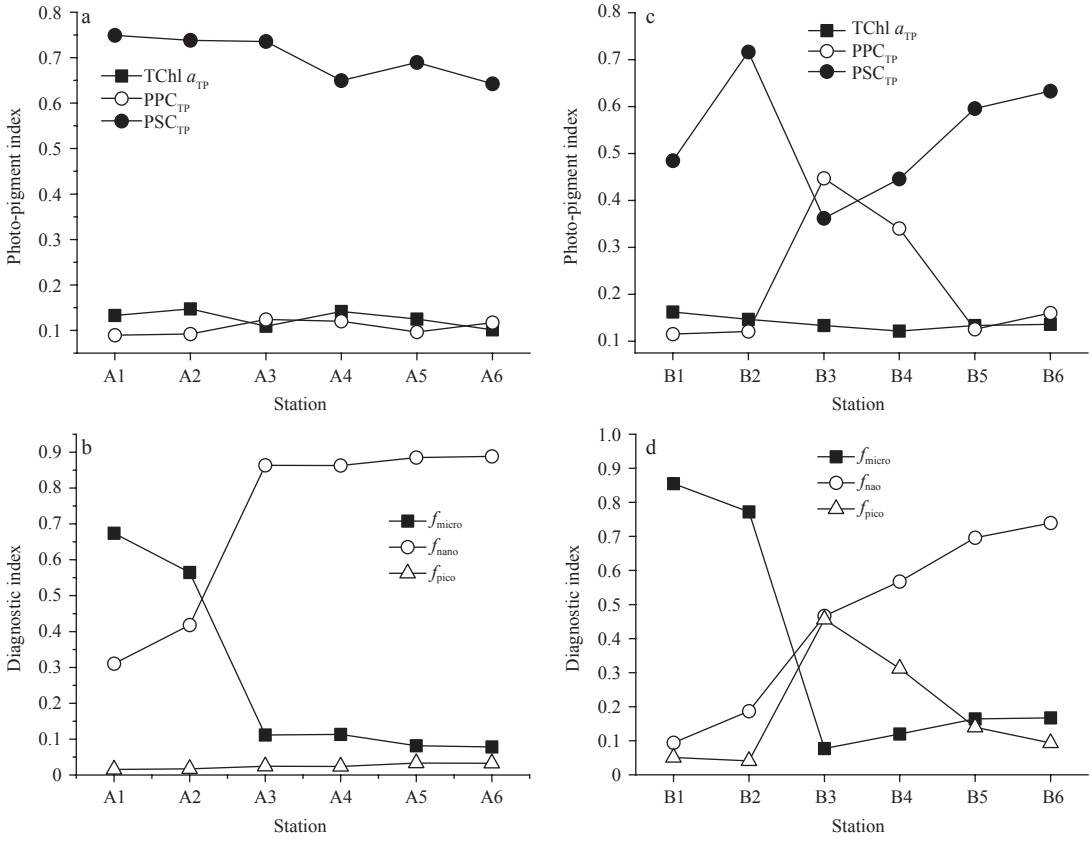

Fig. 4. Spatial distribution of phytoplankton pigment indices.

Table 2. Initial pigment: chlorophyll *a* ratios in the present study

Class/Pigment	Peri	But	Fuco	Neox	Pras	Viol	Hex	Allo	Zea	Lut	Chl *b*	DVChl *a*
Dinoaflgellates	0.838	0	0	0	0	0	0	0	0	0	0	0
Diatoms	0	0	0.947	0	0	0	0	0	0	0	0	0
Haptophytes_8	0	0.688	1.032	0	0	0	0.9	0	0	0	0	0
Haptophytes_6	0	0.016	0.224	0	0	0	1.342	0	0	0	0	0
Chlorophytes	0	0	0	0.029	0	0.078	0	0	0.027	0.129	0.328	0
Cryptophytes	0	0	0	0	0	0	0	0.211	0	0	0	0
Prochlorococcus	0	0	0	0	0	0	0	0	0.334	0	0	1
Synechococcus	0	0	0	0	0	0	0	0	0.358	0	0	0
Prasinophytes	0	0	0	0.093	0.241	0.072	0	0	0.03	0.008	0.953	0
Pelagophytes	0	1.165	0.425	0	0	0	0.008	0	0	0	0	0

Table 3. Final pigment: chlorophyll *a* ratios recalculated by CHEMTAX

Class/Pigment	Peri	But	Fuco	Neox	Pras	Viol	Hex	Allo	Zea	Lut	Chl *b*	DVChl *a*
Dinoaflgellates	0.503	0	0	0	0	0	0	0	0	0	0	0
Diatoms	0	0	0.554	0	0	0	0	0	0	0	0	0
Haptophytes_8	0	0.238	0.257	0	0	0	0.382	0	0	0	0	0
Haptophytes_6	0	0.006	0.096	0	0	0	0.521	0	0	0	0	0
Chlorophytes	0	0	0	0.021	0	0.061	0	0	0.021	0.095	0.233	0
Cryptophytes	0	0	0	0	0	0	0	0.182	0	0	0	0
Prochlorococcus	0	0	0	0	0	0	0	0	0.168	0	0	0.448
Synechococcus	0	0	0	0	0	0	0	0	0.632	0	0	0
Prasinophytes	0	0	0	0.071	0.143	0.052	0	0	0.019	0.005	0.245	0
Pelagophytes	0	0.441	0.176	0	0	0	0.003	0	0	0	0	0

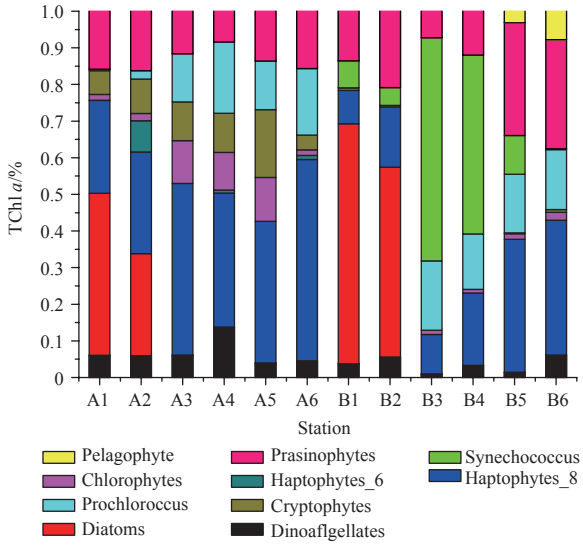

Fig. 5. Relative abundance of phytoplankton groups estimated by CHEMTAX.

contributions varying between 7.23% and 30.78%. Dinoflagellates, cryptophytes, chlorophytes and pelagophytes only contributed a minor part of the Chl *a* biomass in the study area.

4 Discussion

4.1 *Influence of upwelling on phytoplankton composition*

The distribution of phytoplankton in the oceans is governed primarily by the adaption of various communities to changing environmental conditions of temperature, nutrients, irradiance and water column stability (Margalef, 1978). Therefore, the different phytoplankton communities detected will reflect the different water masses and the general oceanographic conditions. Upwelling processes have been reported to have significant impact on phytoplankton community structure in various ecosystems (Ras et al., 2008; Schlüter et al., 2011; Barlow et al., 2007, 2008; Gieskes et al., 1988). In our study area, Chl *a* blooming induced by monsoonal upwelling has been reported through remote sensing (Reddy and Salvekar, 2008; Iskandar et al., 2009, 2010), yet there have been few studies on the impact of upwelling on phytoplankton community structure.

In the present study, the biomass and composition of phytoplankton were contrasting between the upwelling-influenced stations and the offshore regions. In the upwelling-influenced stations (A1, A2, B1 and B2), we detected the high TChl *a* and Fuco concentrations mainly associated with diatoms, and microphytoplankton dominated. This is the typical upwelling feature of a phytoplankton community and is due to the nutrient supply from the deep waters and the prevalence of microphytoplankton in a nutrient-rich and turbulent environment (Marañón, 2015). High phytoplankton biomass and dominance of diatoms have been reported off the Chilean coast of subtropical South Pacific Ocean (Ras et al., 2008), in monsoon-influenced upwelling of the eastern Arabian Sea (Ahmed et al., 2016) and the Banda Sea of Indonesia (Gieskes et al., 1988), in Benguela upwelling region (Barlow et al., 2016), and in the coastal upwelling zone along the western Taiwan Strait (Wang et al., 2016).

By contrast, in the stratified offshore regions, the concentration of Fuco decreased dramatically to very low levels, while the concentrations of Hex and prokaryotic pigments Zea and DVChl *a* increased significantly (Fig. 3). Zea and DV Chl *a* associated with picophytoplankton cyanobacteria and prochlorophytes, respectively, were abundant in highly stratified and nutrient-depleted waters due to their high capacity for nutrient acquisition given by their high surface-to-volume ratios (Raven, 1998). Therefore, although picophytoplankton represented by DVChl *a* and Zea dominated in the vast oligotrophic tropical and subtrop-

ical ocean (Swan et al., 2016), they presented in very low concentrations or were even absent in upwelling zones while showing relatively higher concentrations in offshore regions. Ras et al. (2008) made similar observations in the Chilean upwelling zone.

Overall, Hex associated with haptophytes was the dominant accessory pigment at the SCM in our study, being detected at every station and accounting for 34.49% of the total carotenoids on average. This is consistent with other observations of the world ocean (Gibb et al., 2000; Ras et al., 2008; Swan et al., 2016; Barlow et al., 2016). Hex is regarded as a ubiquitous pigment and has been widely detected in the Atlantic Ocean (Gibb et al., 2000) and the South Pacific Ocean (Ras et al., 2008). The global proportion of marine haptophytes was reported to be 32%±5% in a recent study (Swan et al., 2016). The cosmopolitan distribution of haptophytes might result from their strong capacity for adapting to extreme conditions, enabling them to exploit a wide range of global habitats (Swan et al., 2016; Ras et al., 2008). Hex is the major component of the nanophytoplankton, and explains the dominance of the nanophytoplankton size class in our study.

4.2 *Contributions of PSCs and PPCs at SCM depth*

Marine phytoplankton mainly consists of two functional categories of carotenoids: (1) PSCs and (2) photoprotective carotenoids (PPCs). PSCs are used for light harvesting and PPCs to minimize damage by excess radiation (Porra et al., 1997; Falkowski and Raven, 1997).

Irradiance and nutrient levels are reported to affect the concentrations and ratios of PSCs and PPCs in the phytoplankton community (Trees et al., 2000; Lutz et al., 2003; Gibb et al., 2000; Barlow et al., 2002, 2007; Veldhuis and Kraay, 2004; Brunet et al., 2011). Irradiance is a major driving force for photosynthesis, and increasing the PPCs in high light conditions to prevent photo-oxidative damage to the photosynthetic apparatus is a common mechanism in microalgae. With respect to the nutrient level, PSCs are reported to be more prominent in high-productivity ecosystems in which large phytoplankton dominate (Barlow et al., 2002; Moreno et al., 2012; Madhu et al., 2014); here they can account for 80% of total carotenoids (Gibb et al., 2000). Several observations have reported the dominance of PPCs in the surface oligotrophic waters of the tropical and subtropical Atlantic, Indian and Pacific Oceans (e.g., Gibb et al., 2000; Barlow et al., 2007). While as temperatures and irradiance declined and nutrients increased, there was a significant increase in the proportion of PSCs (Araujo et al., 2017). In high-latitude temperate waters and the Canary Current upwelling system, the total carotenoid budget was dominated by PSCs (Gibb et al., 2000). PPCs were high where nitrate concentrations were less than 0.1 mg/m^3, but at levels greater than 0.1 mg/m^3, PSCs and Chl *a* dominated the pigment pool (Barlow et al., 2007).

In general, high irradiance and low nutrients tend to increase the proportion of PPCs, while PSCs were prominent in low irradiance, low temperature and high nutrient conditions. In the present study, at the subsurface chlorophyll maximum depth, and under conditions of low temperature and irradiance and sufficient nutrients, phytoplankton biomass was elevated, with PSCs being the largest component of the pigment pool, even exceeding the proportion of Chl *a*. This pattern is in close accordance with previous observations. The contribution of PSCs and PPCs, adjusting their pigment pool at the SCM depth, can be seen as phytoplankton adaption strategies to changing environmental conditions.

5 Conclusions

Upwelling occurs on the coast of Java between June and October, forced by local alongshore winds associated with the southeasterly monsoon. Based on field observations during September–October 2013, we studied the distribution and composition of phytoplankton assemblages in the subsurface chlorophyll maximum along the south coast of Java and the influence of upwelling.

A total of nineteen phytoplankton pigments were identified using high-performance liquid chromatography, and CHEMTAX analysis associated these to ten major phytoplankton groups. In the coastal area influenced by upwelling, the phytoplankton community was characterized by high Chl *a* and fucoxanthin concentrations, indicating the dominance of diatoms. In contrast, in the offshore area, the Chl *a* and fucoxanthin concentrations declined to very low levels and the community was dominated by haptophytes represented by 19'-Hexanoyloxyfucoxanthin. Accordingly，microphytoplankton was found to be the major size class in the coastal area influenced by upwelling, while nanophytoplankton was most abundant in the offshore area.

Low concentrations of other accessory pigments indicated less contribution from dinoflagellates, prasinophytes, chlorophytes and cryptophytes. Photo-pigment indices revealed that photosynthetic carotenoids (PSCs) were the largest component of the pigment pool, exceeding the proportion of Chl *a*, with the average PSC_{TP} up to 0.62. These distribution trends can mainly be explained by phytoplankton adaption strategies to upwelling and subsurface conditions by changing species composition and adjusting the pigment pool.

Author contributions: Gao Chunlei and Fu Mingzhu contributed equally to this work. Gao Chunlei designed the study and conducted the HPLC pigment analysis; Fu Mingzhu conducted the data analysis and wrote the manuscript; Song Hongjun performed the pigment sampling and filtration; Wang Lei aided with CHEMTAX operation and data interpretation; Wei Qinsheng provided the nutrients concentration data; Sun Ping provided the dominant phytoplankton species data; Zhang Xuelei and Liu Lin provided the overall project management.

References

Ahmed A, Kurian S, Gauns M, et al. 2016. Spatial variability in phytoplankton community structure along the eastern Arabian Sea during the onset of south-west monsoon. Cont Shelf Res, 119: 30–39, doi: 10.1016/j.csr.2016.03.005

Araujo M L V, Mendes C R B, Tavano V M, et al. 2017. Contrasting patterns of phytoplankton pigments and chemotaxonomic groups along 30°S in the subtropical South Atlantic Ocean. Deep-Sea Res Part I, 120: 112–121, doi: 10.1016/j.dsr.2016.12.004

Barlow R G, Aiken J, Holligan P M, et al. 2002. Phytoplankton pigment and absorption characteristics along meridional transects in the Atlantic Ocean. Deep-Sea Res Part I, 49(4): 637–660, doi: 10.1016/S0967-0637(01)00081-4

Barlow R, Gibberd M J, Lamont T, et al. 2016. Chemotaxonomic phytoplankton patterns on the eastern boundary of the Atlantic Ocean. Deep-Sea Res Part I, 111: 73–78, doi: 10.1016/j.dsr.2016.02.011

Barlow R, Kyewalyanga M, Sessions H, et al. 2008. Phytoplankton pigments, functional types, and absorption properties in the Delagoa and Natal Bights of the Agulhas ecosystem. Estuar Coast Shelf Sci, 80(2): 201–211, doi: 10.1016/j.ecss.2008.07.022

Barlow R, Stuart V, Lutz V, et al. 2007. Seasonal pigment patterns of surface phytoplankton in the subtropical southern hemisphere. Deep-Sea Res Part I, 54(10): 1687–1703, doi: 10.1016/j.dsr.2007.06.010

Bonachela J A, Klausmeier C A, Edwards K F, et al. 2016. The role of phytoplankton diversity in the emergent oceanic stoichiometry. Journal of Plankton Research, 38(4): 1021–1035, doi: 10.1093/

plankt/fbv087
Brunet C, Johnsen G, Lavaud J, et al. 2011. Pigments and photoacclimation processes. In: Roy S, Llewellyn C A, Egeland E S, et al, eds. Phytoplankton Pigments: Characterization, Chemotaxonomy and Applications in Oceanography. Cambridge: Cambridge University Press, 445–471
Chai Chao, Jiang Tao, Cen Jingyi, et al. 2016. Phytoplankton pigments and functional community structure in relation to environmental factors in the Pearl River Estuary. Oceanologia, 58(3): 201–211, doi: 10.1016/j.oceano.2016.03.001
Falkowski P G, Raven J A. 1997. Aquatic Photosynthesis. Oxford: Blackwell
Gibb S W, Barlow R G, Cummings D G, et al. 2000. Surface phytoplankton pigment distributions in the Atlantic Ocean: an assessment of basin scale variability between 50°N and 50°S. Prog Oceanogr, 45(3–4): 339–368
Gieskes W W C, Kraay G W, Nontji A, et al. 1988. Monsoonal alternation of a mixed and a layered structure in the phytoplankton of the euphotic zone of the Banda Sea (Indonesia): a mathematical analysis of algal pigment fingerprints. Netherlands Journal of Sea Research, 22(2): 123–137, doi: 10.1016/0077-7579(88)90016-6
Grasshoff K, Kremling K, Ehrhardt M. 1999. Methods of Seawater Analysis. 3rd ed. Weinheim: Wiley-VCH, 365–371
Higgins H W, Wright S W, Schlüter L. 2011. Quantitative interpretation of chemotaxonomic pigment data. In: Roy S, Llewellyn C A, Egeland E S, et al, eds. Phytoplankton Pigments: Characterization, Chemotaxonomy and Applications in Oceanography. Cambridge: Cambridge University Press, 257–313
Horii T, Ueki I, Syamsudin F, et al. 2016. Intraseasonal coastal upwelling signal along the southern coast of Java observed using Indonesian tidal station data. J Geophys Res Oceans, 121(4): 2690–2708, doi: 10.1002/2015JC010886
Isada T, Hirawake T, Nakada S, et al. 2017. Influence of hydrography on the spatiotemporal variability of phytoplankton assemblages and primary productivity in Funka Bay and the Tsugaru Strait. Estuar Coast Shelf S, 188: 199–211, doi: 10.1016/j.ecss.2017.02.019
Iskandar I, Rao S A, Tozuka T. 2009. Chlorophyll—a bloom along the southern coasts of Java and Sumatra during 2006. Int J Remote Sens, 30(3): 663–671, doi: 10.1080/01431160802372309
Iskandar I, Sasaki H, Sasai Y, et al. 2010. A numerical investigation of eddy-induced chlorophyll bloom in the southeastern tropical Indian Ocean during Indian Ocean Dipole-2006. Ocean Dyn, 60(3): 731–742, doi: 10.1007/s10236-010-0290-6
Jeffrey S W, Wright S W, Zapata M. 2011. Microalgal classes and their signature pigments. In: Roy S, Llewellyn C A, Egeland E S, et al, eds. Phytoplankton Pigments: Characterization, Chemotaxonomy and Applications in Oceanography. Cambridge: Cambridge University Press, 3–77
Kuswardani R T D, Qiao Fangli. 2014. Influence of the Indonesian Throughflow on the upwelling off the east coast of South Java. Chin Sci Bull, 59(33): 4516–4523, doi: 10.1007/s11434-014-0549-2
Lutz V A, Sathyendranath S, Head E J H, et al. 2003. Variability in pigment composition and optical characteristics of phytoplankton in the Labrador Sea and the Central North Atlantic. Mar Ecol Progr Ser, 260: 1–18, doi: 10.3354/meps260001
Mackey M D, Mackey D J, Higgins H W, et al. 1996. CHEMTAX-a program for estimating class abundances from chemical markers: application to HPLC measurements of phytoplankton. Mar Ecol Progr Ser, 144: 265–283, doi: 10.3354/meps144265
Madhu N V, Ullas N, Ashwini R, et al. 2014. Characterization of phytoplankton pigments and functional community structure in the Gulf of Mannar and the Palk Bay using HPLC-CHEMTAX analysis. Continental Shelf Research, 80: 79–90, doi: 10.1016/j.csr.2014.03.004
Marañón E. 2015. Cell size as a key determinant of phytoplankton metabolism and community structure. Ann Rev Mar Sci, 7: 241–264, doi: 10.1146/annurev-marine-010814-015955
Margalef R. 1978. Life-forms of phytoplankton as survival alternatives in an unstable environment. Oceanol Acta, 1(4): 493–509
Mendes C R B, Odebrecht C, Tavano V M, et al. 2016. Pigment-based chemotaxonomy of phytoplankton in the Patos Lagoon estuary (Brazil) and adjacent coast. Mar Biol Res, 13(1): 22–35, doi: 10.1080/17451000.2016.1189082
Moreno D V, Marrero J P, Morales J, et al. 2012. Phytoplankton functional community structure in Argentinian continental shelf determined by HPLC pigment signatures. Estuar Coast Shelf Sci, 100: 72–81, doi: 10.1016/j.ecss.2012.01.007
Paerl H W, Justić D. 2011. Primary producers: phytoplankton ecology and trophic dynamics in coastal waters. In: Wolanski E, McLusky D, eds. Treatise on Estuarine and Coastal Science. Amsterdam: Elsevier, 23–42
Porra R J, Pfündel E E, Engel N. 1997. Metabolism and function of photosynthetic pigments. In: Jeffrey S W, Mantoura R F C, Wright S W, eds. Phytoplankton Pigments in Oceanography: Guidelines to Modern Methods. Paris: UNESCO Publishing, 85–126
Ras J, Claustre H, Uitz J. 2008. Spatial variability of phytoplankton pigment distributions in the Subtropical South Pacific Ocean: comparison between in situ and predicted data. Biogeosciences, 5(2): 353–369, doi: 10.5194/bg-5-353-2008
Raven J A. 1998. The twelfth Tansley Lecture. Small is beautiful: the picophytoplankton. Funct Ecol, 12(4): 503–513, doi: 10.1046/j.1365-2435.1998.00233.x
Reddy P R C, Salvekar P S. 2008. Phytoplankton blooms induced/sustained by cyclonic eddies during the Indian Ocean Dipole event of 1997 along the southern coasts of Java and Sumatra. Biogeosciences Discussion, 5(5): 3905–3918, doi: 10.5194/bgd-5-3905-2008
Sartimbul A, Nakata H, Rohadi E, et al. 2010. Variations in chlorophyll-a concentration and the impact on *Sardinella lemuru* catches in Bali Strait, Indonesia. Prog Oceanogr, 87(1–4): 168–174
Schlüter L, Henriksen P, Nielsen T G, et al. 2011. Phytoplankton composition and biomass across the southern Indian Ocean. Deep-Sea Res Part I, 158(5): 546–556
Susanto R D, Gordon A L, Zheng Quanan. 2001. Upwelling along the coasts of Java and Sumatra and its relation to ENSO. Geophys Res Lett, 28(8): 1599–1602, doi: 10.1029/2000GL011844
Susanto R D, Marra J. 2005. Effect of the 1997/98 El Niño on Chlorophyll a variability along the southern coasts of Java and Sumatra. Oceanography, 18(4): 124–127, doi: 10.5670/oceanog
Swan C M, Vogt M, Gruber N, et al. 2016. A global seasonal surface ocean climatology of phytoplankton types based on CHEMTAX analysis of HPLC pigments. Deep-Sea Res Part I, 109: 137–156, doi: 10.1016/j.dsr.2015.12.002
Trees C C, Clark D K, Bidigare R R, et al. 2000. Accessory pigments versus chlorophyll *a* concentrations within the euphotic zone: a ubiquitous relationship. Limnol Oceanogr, 45(5): 1130–1143, doi: 10.4319/lo.2000.45.5.1130
Uitz J, Claustre H, Morel A, et al. 2006. Vertical distribution of phytoplankton communities in open ocean: An assessment based on surface chlorophyll. J Geophys Res, 111(C8): C08005, doi: 10.1029/2005JC003207
Veldhuis M H W, Kraay G W. 2004. Phytoplankton in the subtropical Atlantic Ocean: towards a better assessment of biomass and composition. Deep-Sea Res Part I, 51(4): 507–530, doi: 10.1016/j.dsr.2003.12.002
Vidussi F, Claustre H, Manca B B, et al. 2001. Phytoplankton pigment distribution in relation to upper thermocline circulation in the eastern Mediterranean Sea during winter. J Geophys Res, 106(C9): 19939–19956, doi: 10.1029/1999JC000308
Wang Yu, Kang Jianhua, Ye Youyin, et al. 2016. Phytoplankton community and environmental correlates in a coastal upwelling zone along western Taiwan Strait. J Mar Syst, 154: 252–263, doi: 10.1016/j.jmarsys.2015.10.015
Wright S W, Ishikawa A, Marchant H J, et al. 2009. Composition and significance of picophytoplankton in Antarctic waters. Polar Biol, 32(5): 797–808, doi: 10.1007/s00300-009-0582-9
Wright S W, Jeffrey S W. 2006. Pigment markers for phytoplankton

production. In: Volkman J K, ed. Marine Organic Matter: Biomarkers, Isotopes and DNA. Berlin: Springer, 71–104

Wyrtki K. 1962. The upwelling in the region between Java and Australia during the south-east monsoon. Australian Journal of Marine and Freshwater Research, 13(3): 217–225, doi: 10.1071/MF9620217

Xue Liang, Wang Huiwu, Jiang Liqing, et al. 2016. Aragonite saturation state in a monsoonal upwelling system off Java, Indonesia. J Mar Syst, 153: 10–17, doi: 10.1016/j.jmarsys.2015.08.003

Zapata M, Garrido J L. 1991. Influence of injection conditions in reversed-phase high-performance liquid chromatography of chlorophylls and carotenoids. Chromatographia, 31(11–12): 589–594

Zapata M, Jeffrey S W, Wright S W, et al. 2004. Photosynthetic pigments in 37 species (65 strains) of Haptophyta: implications for oceanography and chemotaxonomy. Mar Ecol Progr Ser, 270: 83–102, doi: 10.3354/meps270083

Zapata M, Rodríguez F, Garrido J L. 2000. Separation of chlorophylls and carotenoids from marine phytoplankton: a new HPLC method using a reversed phase C^8 column and pyridine-containing mobile phases. Mar Ecol Progr Ser, 195: 29–45, doi: 10.3354/meps195029